Catalysis Today 144 (2009) 149–153

Contents lists available at ScienceDirect

Catalysis Today

journal homepage: www.elsevier.com/locate/cattod

Adsorption and photo-oxidation of 3,4-dihydroxy-cinnamic acid on TiO_2 films

Rossano Amadelli *, Andrea Maldotti, Luca Samiolo

ISOF-CNR and Dipartimento di Chimica, Università degli Studi di Ferrara, Via L. Borsari 46, 44100 Ferrara, Italy

ARTICLE INFO

Article history:
Available online 5 February 2009

Keywords:
3,4-Dihydroxy-cinnamic acid
Photo-oxidation
Titanium dioxide
Films
Adsorption

ABSTRACT

The photo-oxidation of 3,4-dihydroxy-cinnamic acid (DHCA) is investigated on TiO_2 films prepared from commercial Degussa P-25 (FP25 films) and from colloidal TiO_2 prepared by the sol–gel method (FSG films). Photo-oxidation rates have been found to be inversely correlated to the amount of adsorbed species. The extent of adsorption increases as the solution pH increases from 1 to 4 and is more pronounced in the case of FP25 samples for which the amount of adsorbed species is 2.7×10^{-10} mol cm^{-2}, i.e. about threefold higher than for the FSG case. Analysis of DHCA adsorption on TiO_2 suspensions provided information complementary to that collected on films. Diffuse reflectance UV–visible and FTIR spectra of adsorbed DHCA are conspicuously different for the two types of films.

1. Introduction

Interest in semiconductor photocatalysis, and on TiO_2 in particular, is ever growing as witnessed by an impressively large body of research in this field in recent years. The discipline is heading fast toward applications in the field of pollutants abatement [1–3] and significant progress is also being made on the use of semiconductor photocatalysis for synthetic purposes [4,5].

In the present work we examine the TiO_2 photocatalysed oxidation of trans-3,4-dihydroxy-cinnamic acid (henceforth abbreviated as DHCA) as a representative of phenolic acids that are present in wastewaters from olive oil industry. The large content in polyphenolic compounds represents a serious environmental contamination whose remediation has been the target of several recent investigations by different methods, including photocatalysis [6–8] and electrocatalysis [9,10]. On the other hand, the reactivity of polyphenols is interesting as they are important components of natural matter and are well known for their physiological effects due to their antioxidative characteristics [11,12].

The investigations reported in the present work have been carried out on TiO_2 films and provide evidence of the importance of substrate adsorption in the overall reaction mechanism. In principle, DHCA can adsorb onto TiO_2 through interaction of the –COOH and/or through the vicinal OH functional groups and, in this connection, one should note that adsorption of carboxylic acids as well as of catechol has been the object of publications by several authors [13–17].

2. Experimental

2.1. Chemicals

All chemicals including trans-3,4-dihydroxy-cinnamic acid and titanium isopropoxide were obtained from Aldrich and used as received. Commercially available TiO_2 employed was Degussa P-25 (80% anatase and 20% rutile) and, in some experiments, Tayca AMT 100 (pure anatase). The characteristics of the first are a surface area of 50 m^2 g^{-1} and particle size of 24 nm (anatase) and 37 nm (rutile); those of AMT 100 are a surface area of 280 m^2 g^{-1} and particle size of 6 nm.

2.2. Photocatalysts preparation

We have conducted experiments with films prepared from commercial TiO_2 (Degussa P-25) (designated herein as FP25) and nanocrystalline TiO_2 prepared by the sol–gel method starting from titanium isopropoxide (designated herein as FSG).

For the preparation of FP25 films, 3 g of TiO_2 P-25 were dispersed in water (6 ml) and carefully mixed so as to obtain a uniform paste. Acetylacetone (300 μl) and Triton X-100 (100 μl) were then added and after mixing thoroughly in a mortar, the paste was spread on a microscope glass slide within Scotch tape frames, using the "doctor blade technique" [18] and, after drying in air, fired at 450 °C for 30 min.

The preparation of FSG films followed the procedure described by Boschloo and Fitzmaurice [19] starting from colloidal dispersion of TiO_2 nanocrystals, prepared by hydrolysis of titanium

* Corresponding author.
E-mail address: amr@unife.it (R. Amadelli).

0920-5861/$ – see front matter © 2009 Elsevier B.V. All rights reserved.
doi:10.1016/j.cattod.2008.12.020

isopropoxide. The dispersion in 0.1 M HNO_3 was then stirred at 80 °C for 8 h and autoclaved overnight at 150 °C for 12 h, whereupon the initial particle size of the anatase TiO_2 nanocrystals increased from 4–6 to 8–10 nm, as verified from TEM measurements. The obtained dispersion was concentrated, Carbowax 2000 (methoxypolyethylene glycol) added (40% by weight of TiO_2), and the resulting sol stirred overnight. The sol was then spread on glass as described above and, after drying in air, fired at 450 °C for 30 min. The procedures could be optimised so as to obtain films with a geometric area of 1.95 cm^2. We also checked that the weight of the films was the same (4.2 mg) for FP25 and FSG, within a 5% experimental error. The corresponding thickness was 5.5 μm, calculated on the basis of weight and density of TiO_2.

2.3. Characterisation

XRD measurements were recorded on a Bruker model D8 Advance instrument using the CuKα filtered radiation and a graphite monochromator. The data showed that for all samples the crystalline structure corresponded to pure anatase.

Analyses of DHCA solutions, whose pH was always rigorously measured, were carried out by UV–visible spectroscopy, on a Kontron Uvikon 943 spectrophotometer while UV–visible reflectance data were obtained on a Jasco V-570 instrument.

A FTIR Nicolet 510P spectrometer was used to record diffuse reflectance FTIR spectra. For these experiments, at least 4 films were first equilibrated in DHCA solution at fixed pH values in the dark then washed with methanol and dried in a stream of dry air. Finally, the TiO_2 deposits were carefully scratched from the surface and the powder collected was mixed with dry KBr.

Surface roughness measurements were carried out as described by Xagas et al. [20] using (4,4′-dicarboxy-2,2′-bipyridine) (thiocyanato)ruthenium^{II} [$Ru(L_2(NCS)_2$]. The roughness (real area/geometric area) values obtained are 690 and 550 for FP25 and FSG, respectively. The value for FP25 is in agreement with Xagas et al. We also performed tritium exchange measurements to buttress the data obtained with the dye, and the results are reported in Fig. 1. The films were exchanged in tritium water for 48 h, then washed with dry acetone to remove physisorbed water before measuring the tritium release into the scintillator liquid (Imstagel) using a Tricarb 300C Packard liquid scintillation instrument. The results reported in Fig. 1 show that tritium release from a FSG film is higher by a factor of 1.6 with respect to FP25, and since the ratio of surface roughness factors is 1.25, the tritium data apparently reflect surface area, implying that the degree of surface hydroxylation is comparable for the two samples.

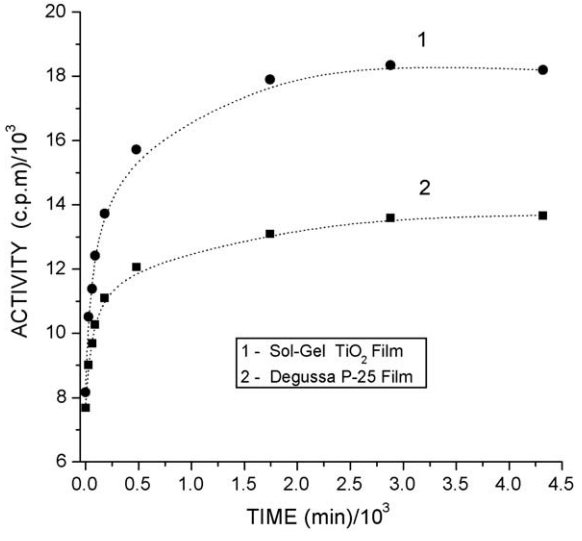

Fig. 1. Tritium exchange kinetic curves for films prepared from sol–gel TiO_2 (FSG) (1) and from Degussa P-25 TiO_2 (FP25) (2).

2.4. Photocatalytic experiments

Experiments were conducted in small Pyrex semi-cylindrical reactors, with a flat window, containing 3 ml of the test solution. The films were immersed in this solution, vertically positioned at a distance of 2 mm from the flat optical window and externally irradiated using a medium pressure mercury lamp (Helios Italquartz) equipped with a Oriel UG-1 band-pass filter (290–400 nm, with 75% transmission at 350–360 nm), interposed between the reactor and the lamp. Experimentally, the lamp was positioned so that illumination was perpendicular to the optical face, and to the film. The radiant power at the reactor surface was 2.7 mW cm^{-2}.

During the experiment, the solution was stirred with Teflon covered magnetic bar. Oxygenation of the solution was assured by maintaining the reactor under pure O_2 at 1 atm. The reactor and the lamp were cooled by fan and the temperature of the test solutions at the end of the irradiation experiments never exceeded 30 °C. Photochemical experiments were also carried out on DHCA in the absence of TiO_2 in order to check that no direct photochemical processes took place.

3. Results and discussion

3.1. Adsorption effects

Strong adsorption of DHCA on both FP25 films and FSG films can be observed qualitatively upon exposure of the films to solutions of the acid as they become coloured. For initial concentrations of DHCA >0.1 mmol L^{-1}, we could measure quantitatively and reproducibly the moles adsorbed from UV–visible spectra of the solution, following the absorbance decrease of two bands located in the range from 285 to 320 nm after 1 h equilibration of the films in the dark [21]. The results show that adsorption of DHCA (initial concentration 0.3 mmol L^{-1}) on both FP25 and FSG films is pH dependent and reaches a maximum at a value of 4, which remains constant up to pH 7. Measurements at still higher pH values were not done since we observed that DHCA solutions became unstable.

Reasonably, the above results are explained by partial carboxylic group dissociation (pK_a of the acid is 4.4), as pointed out for the case of other carboxylic acids [22]. The pH dependence of adsorption is more pronounced in the case of FP25 samples for which, at pH 4, the amount of adsorbed species is 2.7×10^{-10} mol cm^{-2} which is about threefold higher than for the FSG case. This amount, referred to real film area, were calculated from the initial concentration (C_0) and the concentration after equilibrium in the dark (C_{eq}), using the equation $(C_0 - C_{eq})V$, where V is the volume of the solution.

We sought to gain more insight from adsorption isotherm plots and thus we carried out adsorption experiments as a function of DHCA concentration at fixed pH's. In this case, we then conducted experiments using suspensions of the same catalysts used for the preparation of films because this allowed to extend the concentration range to higher values and gives better reproducibility in the lower range of concentrations. Curves b and c in Fig. 2 are the adsorption isotherms of DHCA on suspensions of TiO_2 P-25 in water at pH 2 and 4, respectively; one observes here that the extent of adsorption increases as pH increase, as for films. This enhanced adsorption can be explained by the contribution of carboxyl group ionisation as acidity decreases.

The plots show a multilayer adsorption as the initial solution concentration (C_0) increases, and one also notices that at pH 2

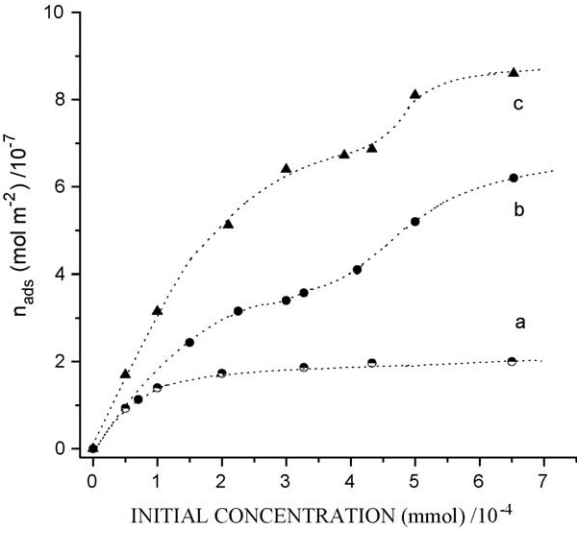

Fig. 2. Adsorption of DHCA on suspensions of TiO_2 Tayca AMT 100 and Degussa P-25. The data for AMT 100 refer to measurements at a solution pH 2 (curve a). The data for P-25 refer to measurements at controlled pH 2 (curve b) and pH 4 (curve c).

(curve b) the second plateau, at the higher C_0 is double with respect to the first which likely indicates the build-up of a second layer of adsorbed species. It is also apparent in Fig. 2 (curve c) that at pH 4 the amount of adsorbed species corresponding to the second plateau is less than twice that of the first. This is likely explained by repulsion effects due to –COOH dissociation that causes formation of a full second layer of adsorbed species to become more difficult.

From similar experiments carried out with the autoclaved colloidal TiO_2 (8–10 nm particle size, see Section 2.2) we do not have evidence supporting multilayer adsorption even in the same range of C_0 values as used for P-25. Unfortunately, experiments were poorly reproducible probably due to incomplete removal of the dispersed phase by filtration and/or to particle aggregation. We assumed, however, that despite some irreproducibility, these semi-quantitative results were correct and that particle size was a possible factor [23,24]. In an alternative experiment we then decided to use commercially available Tayca AMT 100 which is characterised by a small particle size of 6 nm and a specific area of 280 $m^2\ g^{-1}$. Because the area is much larger than that of P-25, the amount of AMT 100 dispersed in the solutions (g L^{-1}) was adjusted so as to compare adsorption isotherms with those for P-25 described above under conditions of equal area, assuming that the area varies linearly with mass of TiO_2. After sonication of the suspensions, the results obtained for a solution at pH 2 (Fig. 2, curve a) are quite reproducible and feature a single adsorption plateau corresponding to an amount of adsorbed moles that is lower than for TiO_2 P-25 at the same pH (cfr. curve b) and, in this respect, the behaviour is analogous to that observed for the sol–gel dispersed oxide. A comparative in-depth analysis of adsorption isotherms can provide valuable information and is worth further separate investigation that cannot be a part of the present study. In the context of the present data, we are led to conclude that particle dimension has an important role in determining the degree of DHCA adsorption and the shape of isotherms. According to Regazzoni et al. [13], there is a limited number of surface titanium ions at the crystal edges and corners that present the highest affinity for adsorbing ligands. One should probably mention the possible effect on adsorption of the rutile component in P-25. However, a 20% rutile in this catalysts does not provide a plausible explanation of the large difference compared to AMT 100, unless the rutile phase totally controls the adsorption process. We then believe that results are better explained on the basis of particles size as the main factor.

3.2. Reflectance UV–visible and FTIR

The results discussed above show that DHCA adsorption on TiO_2 films and suspensions depends quantitatively on pH (in the range from 1.5 to 4) and on the physical–chemical properties of the oxide. In addition, UV–visible diffuse reflectance measurements (Fig. 3) reveal that the interaction of DHCA with the surface of FP25 and FSG TiO_2 film samples gives rise to strikingly different spectra. These have been recorded after equilibration of the films in solutions of 0.5 mmol L^{-1} DHCA at pH 4, where the amount of adsorbed species is maximum. DHCA adsorbed on a FP25 film presents a rather structure-less band that extends into the visible region of the spectrum (Fig. 3, curve 1′), while the analogous spectra on FSG films (Fig. 3, curve 2′) feature a more defined band with a maximum at ∼352 nm tailing into the visible region. A similar band, with a peak at 350 nm, is seen to grow upon addition of increasing amounts of DHCA to ethanol solutions of titanium (IV) isopropoxide; conversely, no such band is observed on addition of cinnamic acid. Coordination of the acid to Ti (IV) through the catecholic functionality again appears most likely by comparison with similar studies on chelates formation of DHCA with Al(III) [25].

FTIR measurements on films, confirmed strong DHCA chemisorption, resulting in conspicuous changes in the whole IR region from 1700 to 1000 cm^{-1} (Fig. 4). Interpretation is complicated by the fact that, in contrast to several publications [25–28] reporting on spectroscopic investigations of DHCA chelate formations with ions in solution, there is a lack of analogous information concerning complex formation on surfaces.

In the wavenumber range from 2000 to 1000 cm^{-1}, the DHCA main IR bands seen in the spectra of Fig. 4 are in agreement with literature data [16,27]. Reported bands assignment includes: ν C=C aromatic (1645 cm^{-1}), ν COOH (1620 cm^{-1}), ν C=C aromatic (1530 cm^{-1}), ν ring (1451 cm^{-1}) and ν CO phenol (1221 cm^{-1}).

When it is adsorbed on FP25, new bands appear at 1713, 1493 and 1280 cm^{-1} while, at the same time, several bands in the range from 1500 to 1000 cm^{-1} disappear. The band at 1713 cm^{-1} can be due to COOH upon loss of conjugation in the lateral chain. In the latter case, one could think about some species which is adsorbed

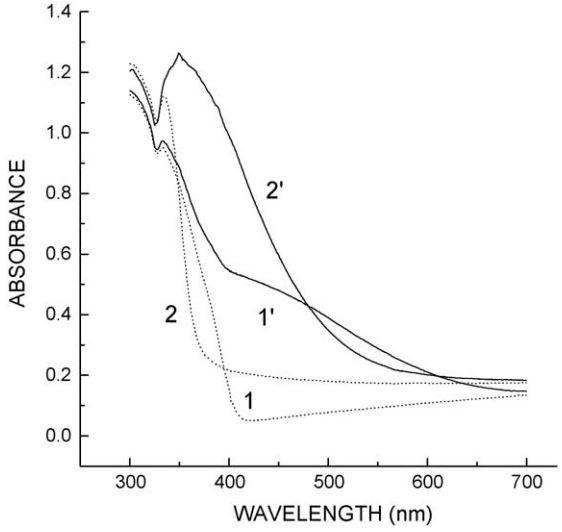

Fig. 3. Diffuse reflectance UV–visible spectra for a FP25 film (1) and a FSG film (2). Curves 1′ and 2′ show the spectra of the films after equilibration in the dark in a 0.5 mmol L^{-1} solution of DHCA at pH 4.

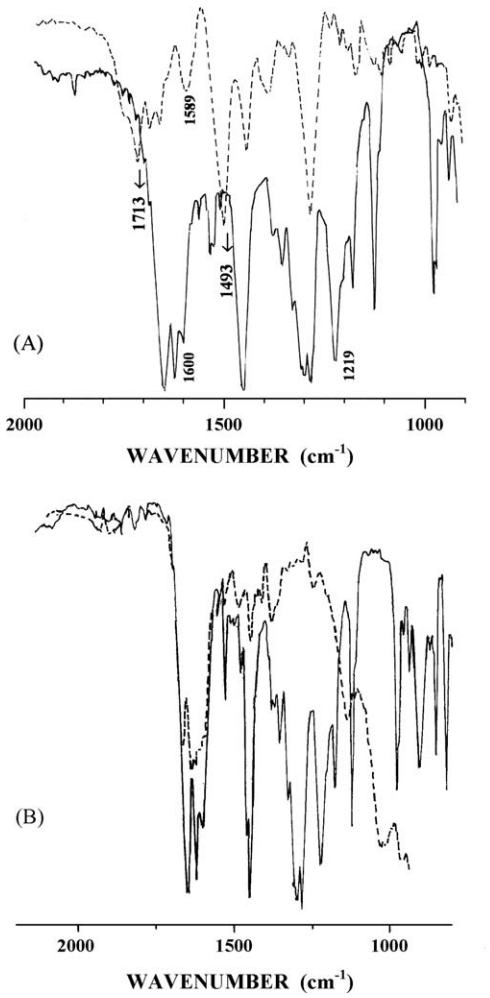

Fig. 4. Comparison of FTIR spectra of DHCA adsorbed on FP25 (A) and FSG (B) films. Solid lines refer to the spectra of DHCA in KBr and dashed lines refer to DHCA adsorbed from 0.5 mmol L^{-1} at pH 4.

through the catechol groups and where also the double bond of the lateral chain interacts with the surface.

Grimes et al. [6] have convincingly proved the importance of the alkene double bond by showing that the adsorption degree of 3,4-dihydroxy-cinnamic acid on TiO_2 is higher than for 3,4-dihydroxy-hydroxycinnamic acid where the lateral chain is saturated. The fact that all functional groups of the molecule seem more or less involved in the adsorption process on this catalysts suggests that adsorbed species essentially lie flat on the surface and would possibly form a dimer with a solution phase DHCA molecule, in keeping with the adsorption isotherms of Fig. 2.

Formation of quinonic species is also a possibility. In fact, Deiana et al. [16] reported the formation of oligomers that exhibit bands at 1710, 1623, 1523, 1443 and 1394 cm^{-1}. In that work, however, those compounds were originated from an interaction of DHCA with Fe(III) that involves charge transfer yielding Fe (II) and DHCA oxidation. In the present case, such situation appears unlikely, and also an oxidation initiated by light can be excluded since experiments have been carried out rigorously in the dark.

The IR spectra of DHCA adsorbed on FSG films (Fig. 4B) show a drastic decrease of the bands below 1500 cm^{-1}, as for the case illustrated in Fig. 4A. At variance with the data on FP25, however, there is seemingly no change in the interval from 1700 to 1500 cm^{-1}, suggesting a poor interaction of the –C═C–COOH molecule moiety with the surface.

3.3. Photo-oxidation

The photo-oxidation of DHCA depends on pH on both types of TiO_2 films and is related to the moles adsorbed even in a range of pH values where the degree of adsorption is lower (pH 1–3), as shown by the data in Table 1. The moles adsorbed per real area (Section 2.3) are given in entries 2 and 4 for FP25 and FSG films, respectively. The initial rate of DHCA photo-oxidation from concentration decay curves as a function of time, normalized to surface area and to the light absorbed by the two types of films (estimated from the films diffuse reflectance data), are given in entries 3 and 5 of the same table. In all cases, the measurement of the adsorbed species and that of initial rates was carried out following 1 h pre-equilibration of the system in the dark. An inspection of the data in Table 1 reveals that on increasing pH the amount of adsorbed species increases while the initial photo-oxidation rate has an inverse relation for both photocatalytic systems examined.

Another test experiment was done where irradiation was started immediately after immersion of the films in the test solution for 1 h. In the first case, the initial concentration is $C = C_0$ (the initial concentration of DHCA in solution) while, in the other case, the concentration is that after dark equilibrium, $C = C_{eq}$, which is lower than C_0 due to adsorption. Then, $C/C_0 = 1$ and $C/C_0 < 1$, respectively, when illumination is started.

By comparison, the initial photo-oxidation rates of 0.5 mmol L^{-1} DHCA at pH 4 were typically twice higher than those obtained after the pre-equilibrium step in the dark, as shown for the case of a FP25 film in Fig. 5. This again confirms that adsorption has an adverse effect which is particularly evident at the short irradiation times.

The relation between adsorption and photocatalytic activity has been the object of several studies, some more closely related to the

Table 1
Adsorption of DHCA (0.5 mmol L^{-1}) on TiO_2 films and normalised (see text) initial photo-oxidation rates r^0, as a function of pH.

pH	$n_a/10^{-10}$ (mol cm^{-2})	$(r^0)^a$	$n_b/10^{-10}$ (mol cm^{-2})	$(r^0)^b$
1.5	1.40	2.30	0.22	2.60
2.0	1.55	1.57	0.40	2.28
2.7	1.68	1.68	0.46	1.96
4.0	2.73	0.85	0.64	1.14

r^0, μmol min^{-1} W^{-1}.
[a] P-25 film.
[b] SG film.

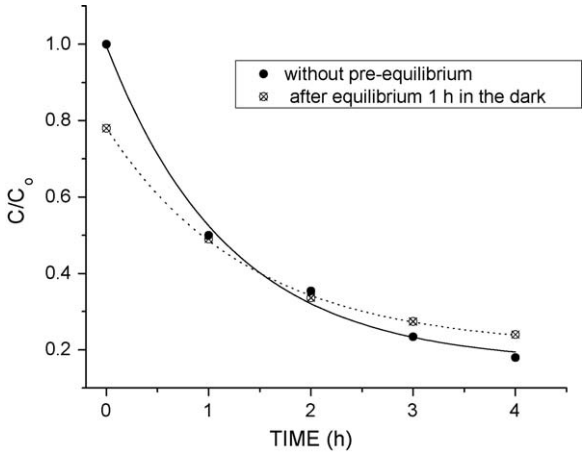

Fig. 5. Normalized concentration (C/C_0) vs. time curves for the photo-oxidation 0.5 mmol L^{-1} DHCA at pH 4 without (solid line) and with pre-equilibrium in the dark (dotted line). See text for explanation.

problem discussed in this paper [e.g. 6,29]. In their investigation on the photocatalytic oxidation of gallic acid on TiO_2 suspensions, Gumy et al. [29] found that initial rates of disappearance correlated with the amount of adsorbed acid. Their data have been obtained using catalysts with different surface area while the approach we followed in this work is based on surface area-normalised results.

There are evident limitations in comparing particle size effects in dispersions and sintered films, however the results discussed above (Table 1) in this section seem to compare with the data of Fig. 2. The films we investigated have comparable macroscopic available areas but are composed of crystallites with rather different size. AFM measurements (not shown) on the FSG sol–gel films, reveal a network of small crystallites together with few larger ones, while the FP25 films are composed of large aggregates mainly. We might invoke an effect of microstructure on adsorption as it is reported to exist in aggregates [23], and as it exists on suspension of particles of different sizes (Fig. 2). In the cited work, Zhang et al. [24] found that adsorption of oxalic and adipic acid shows as much as a 70-fold increase of K_{ads} as particle size decreases. Pettibone et al. [23] in their study of particle size effect on adsorption of the same organic acids on TiO_2 found no evidence that adsorption strength or extent increases with decreasing particle size, and the question is then open to further study.

4. Conclusions

A striking feature of photo-oxidation of 3,4-dihydroxy-cinnamic acid on TiO_2 films is its decreases with increasing adsorption of the acid. Two types of TiO_2 films prepared from a commercial product (Degussa P-25) and from colloidal suspensions of the oxide showed different photoactivity that is related to the extent of adsorption. Films obtained from the colloids feature a higher photoactivity and lower degree of adsorption than those prepared from the commercial oxide.

Since the measured surface area of the two types of films was comparable, differences can be ascribed to the different film texture: a network of small crystallites together with few larger ones is characteristic of the sol–gel films. Complementary data obtained from experiments on DHCA adsorption on commercial TiO_2 suspensions reveal that particle size in an important factor determining the amount of adsorbed species and the shape of adsorption isotherms.

Acknowledgements

The authors acknowledge financial support from CTG-Italcementi and the Italian National Council of research (CNR).

References

[1] M.R. Hoffmann, S.T. Martin, W. Choi, D. Bahnemann, Chem. Rev. 95 (1995) 69.
[2] O.M. Alfano, D. Bahnemann, A.E. Cassano, R. Dillert, R. Goslich, Catal. Today 58 (2000) 199.
[3] O. Carp, C.L. Huisman, A. Reller, Progr. Solid State Chem. 32 (2004) 33.
[4] A. Maldotti, A. Molinari, R. Amadelli, Chem. Rev. 102 (2002) 3811.
[5] G. Palmisano, V. Augugliaro, M. Pagliaro, L. Palmisano, Chem. Commun. 33 (2007) 3425.
[6] S.M. Grimes, L.K. Mehta, H.C. Ngwang, J. Environ. Sci. Health 36 (2001) 599.
[7] S.S. Kim, H.J. Kim, H.J. Lee, S.K. Park, J. Photosci. 10 (2003) 181.
[8] A.M.T. Silva, E. Nouli, N.P. Xekoukoulotakis, D. Mantzavinos, Appl. Catal. B: Environ. 73 (2007) 11.
[9] R. Amadelli, A. De Battisti, D.V. Girenko, S.V. Kovalyov, A.B. Velichenko, Electrochim. Acta 46 (2000) 341.
[10] P. Hapiot, A. Neudeck, J. Pinson, H. Fulcrand, P. Neta, C. Rolando, J. Electroanal. Chem. 405 (1996) 169.
[11] Y. Maegawa, K. Sugino, H. Sakurai, Free Radical Res. 41 (2007) 110.
[12] T. Gao, Y. Ci, H. Jian, C. An, Vib. Spectrosc. 24 (2000) 225.
[13] A.E. Regazzoni, P. Mandelbaum, M. Matsuyoshi, S. Schiller, S.A. Bilmes, M.A. Blesa, Langmuir 14 (1998) 868.
[14] R. Rodriguez, M.A. Blesa, A.E. Regazzoni, J. Colloid Interface Sci. 177 (1996) 122.
[15] C. Minero, F. Catozzo, E. Pelizzetti, Langmuir 8 (1992) 481.
[16] S. Deiana, A. Premoli, C. Senette, Plant Physiol. Biochem. 46 (2008) 435.
[17] S.T. Martin, J.M. Kesselman, D.S. Park, N.S. Lewis, M.R. Hoffmann, Environ. Sci. Technol. 30 (1996) 2535.
[18] C.J. Barbé, F. Arendse, P. Comte, M. Jirousek, F. Lenzmann, V. Shklover, M. Grätzel, J. Am. Ceram. Soc. 80 (1997) 3157.
[19] G. Boschloo, D. Fitzmaurice, J. Electroch. Soc. 147 (2000) 1117.
[20] A.P. Xagas, E. Androulaki, A. Hiskia, P. Falaras, Thin Solid Films 357 (1999) 173.
[21] J. Cunningham, G. Al-Sayyed, J. Chem. Soc. Faraday Trans. 86 (1990) 3935.
[22] P.Z. Araujo, P.J. Morando, M.A. Blesa, Langmuir 21 (2005) 3470.
[23] J.M. Pettibone, D.M. Cwiertny, M. Scherer, V.H. Grassian, Langmuir 24 (2008) 6659.
[24] H. Zhang, R.L. Penn, R.J. Hamers, J.F. Banfield, J. Phys. Chem. B 103 (1999) 4656.
[25] J.P. Cornard, C. Lapouge, J. Phys. Chem. A 108 (2004) 4470.
[26] J.P. Cornard, C. Lapouge, J. Phys. Chem. A 110 (2006) 7159.
[27] P.A.M. Williams, A.C. Gonzalez Baró, E.G. Ferrer, Polyhedron 21 (2002) 1979.
[28] M. Ge, H. Zhao, W. Wang, Z. Zhang, X. Yu, W. Li, J. Biol. Phys. 32 (2006) 403.
[29] D. Gumy, A.G. Rincon, R. Hajdu, C. Pulgarin, Solar Energy 80 (2006) 1376.